Title

Cannabinoid CB2 receptors mediate the anxiolytic-like effects of monoacylglycerol lipase inhibition in a rat model of predator-induced fear

Authors

Ivy, Devon
Palese, Francesca
Vozella, Valentina
et al.

ARTICLE

Cannabinoid CB$_2$ receptors mediate the anxiolytic-like effects of monoacylglycerol lipase inhibition in a rat model of predator-induced fear

Devon Ivy[1], Francesca Palese[1], Valentina Vozella[1], Yannick Fotio[1], Aylin Yalcin[1], Gina Ramirez[1], David Mears[2,3], Gary Wynn[3] and Daniele Piomelli[1,4,5]

The endocannabinoid system is a key regulator of the response to psychological stress. Inhibitors of monoacylglycerol lipase (MGL), the enzyme that deactivates the endocannabinoid 2-arachidonoyl-*sn*-glycerol (2-AG), exert anxiolytic-like effects in rodent models via 2-AG-dependent activation of CB$_1$ cannabinoid receptors. In the present study, we examined whether the MGL inhibitor JZL184 might modulate persistent predator-induced fear in rats, a model that captures features of human post-traumatic stress disorder. Exposure to 2,5-dihydro-2,4,5-trimethylthiazoline (TMT), a volatile chemical that is innately aversive to some rodent species, produced in male rats a long-lasting anxiety-like state that was measured 7 days later in the elevated plus maze test. Systemic administration of JZL184 [4, 8 and 16 mg/kg, intraperitoneal (IP)] 4 h before testing caused dose-dependent inhibition of MGL activity and elevation of 2-AG content in brain tissue. Concomitantly, the inhibitor suppressed TMT-induced fear behaviors with a median effective dose (ED$_{50}$) of 4 mg/kg. A similar behavioral response was observed with another MGL inhibitor, KML29 (4 and 16 mg/kg, IP). Surprisingly, the effect of JZL184 was prevented by co-administration of the CB$_2$ inverse agonist AM630 (5 mg/kg, IP), but not the CB$_1$ inverse agonist rimonabant (1 mg/kg, IP). Supporting mediation of the response by CB$_2$ receptors, the CB$_2$ agonist JWH133 (0.3, 1 and 3 mg/kg, IP) also produced anxiolytic-like effects in TMT-stressed rats, which were suppressed by AM630. Notably, (i) JWH133 was behaviorally ineffective in animals that had no prior experience with TMT; and (ii) CB$_2$ mRNA levels in rat prefrontal cortex were elevated 7 days after exposure to the aversive odorant. The results suggest that JZL184 attenuates the behavioral consequences of predator stress through a mechanism that requires 2-AG-mediated activation of CB$_2$ receptors, whose transcription may be induced by the stress itself.

INTRODUCTION

The endocannabinoid system serves critical regulatory functions in the response to psychological stress [1]. This signaling complex – which is comprised of two cell-surface receptors (CB$_1$ and CB$_2$) and their cognate lipid-derived agonists (anandamide and 2-arachidonoyl-*sn*-glycerol, 2-AG) [2, 3] – was first implicated in the control of stress-coping behaviors by experiments with the compound URB597, a selective inhibitor of the anandamide-degrading enzyme fatty acid amide hydrolase (FAAH) [4, 5]. FAAH inhibition by URB597 was shown to activate serotonergic and noradrenergic neurons in the rat midbrain [6] and to produce beneficial effects in mouse and rat models used to investigate anxiety [4, 7, 8] and depression [6–9]. These effects were shown to require activation of CB$_1$ receptors by endogenously produced anandamide [4, 6] and to depend on brain structures involved in emotional control, such as the basolateral amygdala and the lateral habenula [1]. Human studies have corroborated these preclinical data showing that pharmacological FAAH blockade improves the recall of fear extinction memories and alleviates

stress-induced anxiety in healthy volunteers [10], and that persons carrying the hypofunctional FAAH mutation C385A (Pro129Thr) experience heightened fear extinction and extinction recall [11].

2-AG-mediated endocannabinoid signaling has also been implicated in the control of stress-coping responses [1]. In the central nervous system (CNS), 2-AG is produced upon demand in dendritic spines and activates CB$_1$ receptors on adjacent axon terminals [12]. This retrograde feedback process regulates excitatory and inhibitory transmission throughout the CNS and is terminated by the presynaptic serine hydrolase monoacylglycerol lipase (MGL), which converts 2-AG into arachidonic acid and glycerol [13, 14]. Like FAAH, MGL has emerged as a potential target for anxiolytic drug discovery. For example, testing rats in the elevated plus maze (EPM), Hohmann and collaborators showed that the MGL inhibitor JZL184 produces marked anxiolytic-like effects, which are prevented by the CB$_1$ inverse agonist rimonabant [15]. Similarly, Lichtman and coworkers reported that JZL184 decreases marble burying in mice through a mechanism that requires CB$_1$ activation [16]. Brain regions

[1]Department of Anatomy and Neurobiology, University of California, Irvine, 3103 Gillespie Neuroscience Research Facility, Irvine, CA 92697-4625, USA; [2]Department of Anatomy, Physiology, and Genetics, Uniformed Service University of the Health Sciences, Bethesda, MD, USA; [3]Center for the Study of Traumatic Stress, Department of Psychiatry, Uniformed Service University of the Health Sciences, Bethesda, MD, USA; [4]Department of Pharmaceutical Sciences, University of California, Irvine, Irvine 92697 CA, USA and [5]Department of Biological Chemistry, University of California, Irvine, Irvine 92697 CA, USA
Correspondence: Daniele Piomelli (piomelli@uci.edu)

implicated in the anxiolytic-like actions of JZL184 include the amygdala [17], the dorsolateral periaqueductal gray [18] and the hippocampus [19].

In the present study, we evaluated the effects of MGL blockade in the 2,5-dihydro-2,4,5-trimethylthiazoline (TMT) model of innate predator-induced fear. Adult male rats that are briefly exposed to TMT – a volatile semiochemical that is strongly aversive to some rodent species – develop a persistent anxiety-like state that can be measured in the EPM test [20, 21]. Using this model, we found that administration of JZL184 results in dose-dependent inhibition of MGL activity and elevation of 2-AG content in brain tissue, which are paralleled by suppression of TMT-induced fear. A second MGL inhibitor, KML29, exerted similar effects. Unexpectedly, however, the behavioral response to JZL184 was abolished by CB$_2$, not CB$_1$ receptor blockade. Consistent with a critical involvement of CB$_2$ receptors, the selective agonist JWH133 produced marked anxiolytic-like effects in TMT-stressed rats, which were countered by the CB$_2$ antagonist AM630. Finally, exposure to TMT was required for the anxiolytic-like properties of JWH133 to be expressed, and was accompanied by heightened transcription of the CB$_2$ gene in the prefrontal cortex.

MATERIALS AND METHODS
Animals
We used 274 male Sprague-Dawley rats (Charles River, Wilmington, MA), weighing 225–250 g (8–9-week old) upon arrival. They were housed in groups of 4 and maintained on a 12 h light-dark cycle (lights on at 06:30) under constant conditions of temperature (22 ± 2 °C) and relative humidity (55–60%). Food and water were available *ad libitum*. All procedures were approved by the Institutional Animal Care and Use Committee at the University of California, Irvine, and were carried out in accordance with the National Institute of Health guidelines for the care and use of experimental animals.

Chemicals
TMT was purchased from BioSQR (Sarasota, FL). AM630, JWH-133, JZL184, KML29 and rimonabant were from Cayman (Ann Arbor, MI). All analytical solvents were of the highest grade commercially available.

Drug preparation
We dissolved JZL184 in polyethylene glycol 400 (PEG-400)/Tween-80 (4:1, vol/vol) (Sigma-Aldrich, St. Louis, MO). KML29 was dissolved in PEG-400 and sonicated for 20 min at 30 °C. Rimonabant was dissolved in PEG-400/Tween-80/sterile 0.9% sodium saline (1:1:18, vol/vol/vol) and sonication for 10 min at 30 °C. AM630 was dissolved in dimethylsulfoxide (DMSO)/Tween-80/0.9% sodium saline (1:1:18, vol/vol/vol). JWH-133 was dissolved in DMSO/0.9% sodium chloride (1:9, vol/vol).

TMT exposure
Rats were handled for 5 consecutive days in random order for 2 min each and were placed for 15 min in plastic exposure boxes (30 × 22 × 22 cm) containing gauze squares (5 × 5 cm) doused with saline (0.9% sodium chloride, 50 μL). Beginning on day 3, rats received daily injections of sterile saline (1 mL/kg, IP). At the end of this habituation period, the animals were placed for 20 min in boxes containing gauze squares doused with either saline or TMT (5.8 mM, 50 μL) and then returned to their cages.

EPM test
We described in detail the EPM apparatus and protocol elsewhere [22]. Behavioral tests were conducted between 10:30 and 14:30 h. The open arms of the maze were illuminated at 150–170 lux and the closed arms at 40-50 lux. Animal performance were recorded using the Debut video capture software. Observers blind to

treatment conditions measured the amount of time animals spent in open arms, closed arms and center, as well as number of open arm entries, closed arm entries, and both number and time exploring in stretch-attend postures and open arm ("unprotected") head dips. The anxiety index was calculated by the following formula:

$$\text{Anxiety Index} = 1 - \frac{\left(\frac{\text{time spent in open arms}}{\text{total time}}\right) + \left(\frac{\text{number of open arm entries}}{\text{total entries}}\right)}{2}$$

The standard EPM index was calculated by the formula:

$$\text{EPM Index} = 100 \times \frac{\text{Time spent in open arms}}{(\text{time spent in open arm} + \text{time spent in closed arm})}$$

Feeding and motor behavior
We habituated animals to the test cages for 3 days prior to trials. Food intake and motor behavior were recorded simultaneously using an automated system (TSE, Bad Homburg, Germany), starting at the onset of the dark phase (18:30) and lasting for 24 h. The system, protocol and feeding parameters surveyed were those previously described [23]. Data were analyzed as total food intake per kg of body weight and as cumulative food intake (g/kg) over 24 h. Motor activity was recorded using an X-Y matrix of infrared sensors, and is reported as "beam breaks" per hour.

MGL enzyme activity assay
We weighed rat hippocampi and homogenized them in ice-cold Tris-HCl buffer (50 mM, pH 7.5, 1:10 weight/vol). Homogenates were centrifuged for 10 min at 1000 × g at 4 °C. Supernatants were collected, and protein concentrations measured using the bicinchoninic acid (BCA) assay test (Pierce, Rockford, IL). To measure MGL activity, we incubated tissue homogenates (7.5 μg protein) at 37 °C for 30 min in 0.5 mL of Tris-HCl (50 mM, pH 7.5) containing fatty acid-free bovine serum albumin (0.05% weight/vol; Millipore-Sigma, Burlington, MA) and 10 μM 2-oleoyl-*sn*-glycerol. The reactions were stopped with 1 mL of ice-cold methanol containing 5 nmol heptadecanoic acid. 2 mL of chloroform and 0.5 mL of water were added to the samples, which were subsequently centrifuged at 2000 × g at 4 °C for 15 min. The organic layers were collected and evaporated under nitrogen. The pellets were dissolved in 1 mL of methanol and transferred into 1.5 mL glass vials for liquid chromatography/mass spectrometry (LC/MS) analysis. These were performed using an Agilent 1200 LC system coupled to a G6410A triple quadrupole MS detector (Agilent Technologies, Santa Clara, CA) and equipped with an XBD Eclipse C18 (2.1 mm × 50 mm, 1.8 μm particle size) column (Agilent Technologies). The mobile phase consisted of 0.25% acetic acid and 5 mM ammonium acetate in methanol as solvent A and 0.25% acetic acid and 5 mM ammonium acetate in water as solvent B. Lipids were eluted in 6 min under a linear gradient condition of: 6.2% solvent A and 93.8% solvent B from 00:00-02:00 min (0.5 mL/min flow rate), 5.0% solvent A and 95% solvent B from 02:01-03:50 min (0.8 mL/min flow rate), and 11.0% solvent A and 89% solvent B from 03:51-06:00 min (0.8 mL/min flow rate). The mass spectrometer was operated in the negative electrospray ionization (ESI) mode and quantification was performed by monitoring the mass-to-charge ratio (*m/z*) of deprotonated molecular ions [M-H]$^-$ in the selected ion-monitoring mode. Capillary voltage was set to 4 kV, fragmentor voltage was 100 V; nitrogen was used as drying gas at a flow rate of 13 l/min and at a temperature of 350 °C. Nebulizer pressure was set at 60 psi.

Lipid analyses
We homogenized rat hippocampi (3–5 mg) in ice-cold methanol (1 mL) containing 0.5 nmol [^{2}H$_5$]-2-AG as internal standard. Lipids were extracted with chloroform (2 mL), and the extracts washed

with water (1 mL). After centrifugation at $2850 \times g$ at 4 °C the organic phases were collected and transferred into new vials. The solvent was evaporated under nitrogen and reconstituted in chloroform (2 mL). Lipids were fractionated by open-bed silica gel column chromatography (silica gel G, 60-Å 230-400 Mesh; ASTM; Whatman, Clifton, NJ). 2-AG was eluted from the column with 2 mL of 9:1 chloroform:methanol. The eluates were collected, evaporated under nitrogen, and reconstituted in 0.1 mL methanol:chloroform (9:1, vol/vol). Analyses were performed using an Agilent 1200 LC system coupled to a G6410A triple quadrupole MS detector (Agilent Technologies) and equipped with an XBD Eclipse C18 column (3.0 mm × 50 mm, 1.8 μm). The mobile phase consisted of 0.25% acetic acid and 5 mM ammonium acetate in water as solvent A, and 0.25% acetic acid and 5 mM ammonium acetate in methanol as solvent B. Lipids were eluted under isocratic conditions with 80% B in 7.00 min followed by a column wash of 95% B from 7.01 to 9 min. The flow rate was 0.5 mL/min and the injection volume 5 μL. Column temperature was 40 °C. The mass spectrometer was operated in the positive ESI mode and quantification was performed using the following multiple reaction-monitoring transitions: m/z 379 > 287 for 2-AG; m/z 384 > 287 for [^{2}H$_5$]-2-AG; m/z 401 > 401 for [2-AG]Na$^+$; m/z 406 > 406 for [^{2}H$_5$-2-AG]Na$^+$. Capillary voltage was 4 kV and fragmentor voltage was 135 V. Collision energy varied from 10 to 20 eV. Nitrogen was used as a drying gas at a flow rate of 12 L/min at 350 °C. Nebulizer pressure was set at 50 psi.

Real-time quantitative PCR
We anesthetized rats with isoflurane and perfused ice-cold sterile saline through the left heart ventricle for 2 min before collecting the brains. We prepared total RNA from tissue samples (3–5 mg) using the Ambion PureLink RNA minikit (Life Technologies, Carlsbad, CA, USA) as directed by the supplier. Samples were treated with DNase (PureLink DNase, Life Technologies) and cDNA synthesis was carried out using the High capacity cDNA Reverse Transcription kit (Life Technologies) according to the manufacturer's protocol and using purified RNA (2 μg). First-strand cDNA was amplified using the TaqMan 5′ nuclease activity from the TaqMan Universal PCR Master Mix, and fluorogenic probes (Life Technoogies) or using Sybrgreen mix (Qiagen, Germantown, MD), and custom oligonucleotide primers (Life Technologies). Gene-specific CB$_1$, actin and GAPDH primers for TaqMan assays were purchased from Life Technologies. CB$_2$, actin and GAPDH were custom designed using the following sequences: CB$_2$ forward CCG AGG CCA CCC AGC AAA CA; CB$_2$ reverse CCG CCA TTG GAG CCG TTG GT; Actin forward AAG TCC CTC ACC CTC CCA AAA G; Actin reverse AAG CAA TGC TGT CAC CTT CCC; GAPDH forward CAA CTC CCT CAA GAT TGT CAG CAA; GAPDH reverse GGC ATG GAC TGT GGT CAT GA. Quantitative PCR was performed in 96-well PCR plates and run at 95 °C for 10 min, followed by 40 cycles, each cycle consisting of 15 s at 95 °C and 1 min at 60 °C, using a Stratagene MX 3000p instrument (Agilent). Copy numbers of cDNA targets were quantified of the point during cycling when the PCR product was first detected. CB$_1$ transcripts were detected at 19-23 cycles (depending on brain area), while CB$_2$ transcripts were detected between cycle 24 and 27. The BestKeeper software [24] was used to determine expression stability and geometric mean of two different housekeeping genes (Actin and GAPDH). ΔCt values were calculated by subtracting the Ct value of the geometric mean of these housekeeping genes from the Ct value for the genes of interest. The relative quantity of genes of interest was calculated by the expression $2^{-\Delta\Delta Ct}$. Results are reported as fold induction over control.

Statistical analyses
Results are presented as mean ± SEM. All the data were analyzed by Levene's test and met the assumption of homogeneity of variances ($P > 0.1$). Data were analyzed by Student's unpaired t-test followed by Bonferroni's multiple correction, one-way ANOVA or two-way ANOVA followed by Newman–Keuls multiple comparison test, as appropriate. Differences between groups were considered statistically significant at values of $P < 0.05$.

RESULTS
Dose-range finding studies
As questions remain about the potency of JZL184 across rodent species [25], we determined the effects of ascending doses of the inhibitor (4, 8 and 16 mg/kg, IP) or its vehicle on MGL activity and 2-AG content in extracts of hippocampal tissue from adult male rats ($n = 4$–5 per group). Four h after JZL184 injections, MGL activity was dose-dependently decreased [F (3, 76) = 19.93; $P < 0.0001$] and, concomitantly, 2-AG content was increased in the extracts [F (3, 27) = 3.455; $P = 0.0303$; Supplementary Fig. 1].

Evaluation of potential behavioral confounders
JZL184 reduces locomotion in mice [26]. Since this effect may interfere with the interpretation of EPM data, we treated single-housed rats with the inhibitor (4, 8 and 16 mg/kg, IP) and monitored locomotor activity in a familiar environment for 24 h starting 2 h after drug injections ($n = 6$ per group). As illustrated in Supplementary Fig. 2, JZL184 caused a dose-dependent reduction in activity [F (3, 18) = 12.88; $P < 0.0001$; Supplementary Fig. 2A], which returned to baseline 4 h later (Supplementary Fig. 2B). In a parallel assessment of circadian feeding, we found that JZL184 did not alter cumulative food intake (Supplementary Fig. 3A), average meal size (Supplementary Fig. 3B), post-meal interval (Supplementary Fig. 3C) or satiety ratio (Supplementary Fig. 3D) at any time following administration. Based on these initial observations, we conducted all subsequent experiments using a JZL184 dose range of 4 to 16 mg/kg and a behavioral testing time of 4 h post injection.

Effects of JZL184 in non-stressed rats
In rats that were not previously challenged with TMT, JZL184 (16 mg/kg) did not alter behavioral performance in the EPM test (Fig. S4), when such test was conducted under mildly stressful conditions (i.e., low ambient light, see Materials and Methods). This result is consistent with published data suggesting that environmental aversiveness is necessary to unmask the anxiolytic-like effects of JZL184 [15].

Anxiolytic-like effects of MGL-inhibition in TMT-stressed rats
We exposed rats to TMT and assessed fear-related behaviors in the EPM 7 days later [17]. As in the previous experiment, the tests were run under mildly aversive environmental conditions (i.e., low ambient light). Treatment with JZL184 produced a robust, dose-dependent anxiolytic-like effect, as assessed by increased time in open arms [F (3, 28) = 4.319; $P = 0.0127$; Fig. 1a], reduced time in closed arms [F (3, 28) = 5.207; $P = 0.0055$; Fig. 1b], lowered the anxiety index (F (3, 28) = 4.590; $P = 0.0098$; Fig. 1c) and increased the EPM index (Supplementary Table 1). Separate experiments with a structurally distinct MGL inhibitor, KML29 [27], produced similar results: 4 h after KML29 administration, we detected a dose-dependent anxiolytic-like effect in TMT-exposed rats, with an increase in time spent in open arms [F (2, 20) = 7.068; $P = 0.0048$; Fig. 1d], lower anxiety index [F (2, 20) = 7.061; $P = 0.0048$; Fig. 1f] and higher EPM index (Supplementary Table 1). Of note, while JZL184 treatment decreased number of stretch-attend postures [F (3, 28) = 5.246; $P = 0.0053$; Supplementary Fig. 5A and increased number of exploratory head dips [F (3, 28) = 5.290; $P = 0.0051$; Supplementary Fig. 5B], KML29 only showed a non-significant trend in both parameters (Supplementary Fig. 5C, D). The results indicate that pharmacological blockade of intracellular MGL activity alleviates fear-related behaviors in TMT-stressed rats. At the dosages used, JZL184 appeared to be more effective than KML29.
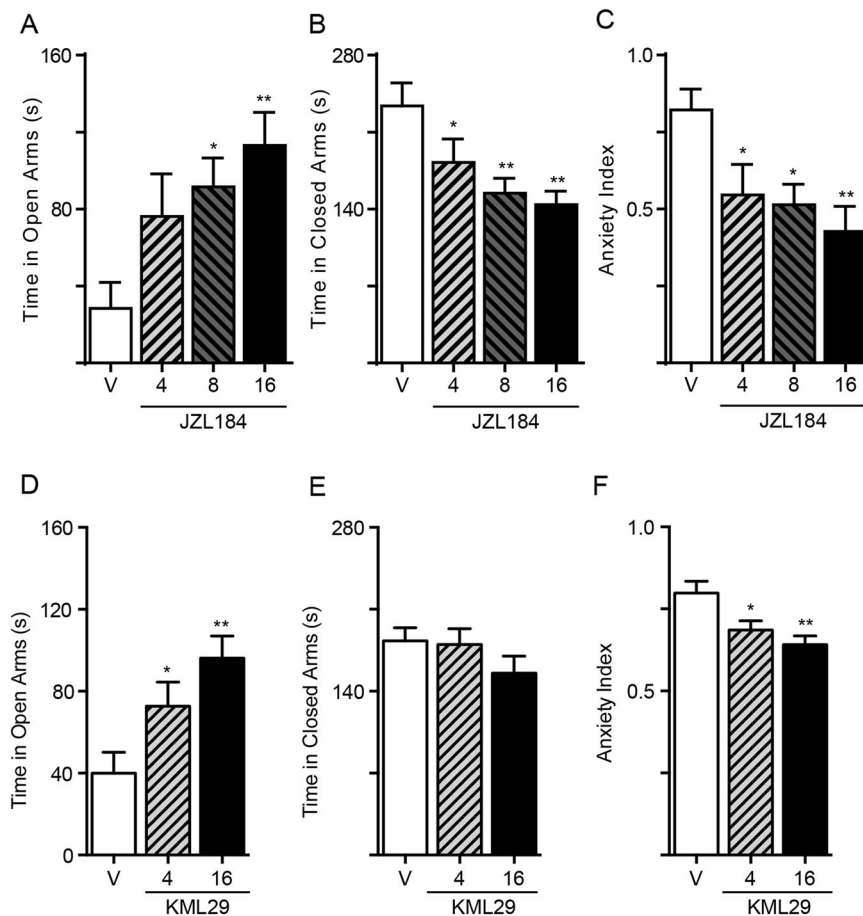
Fig. 1 Effects of JZL184 and KML29 on anxiety-related behaviors in TMT-stressed rats. a–c JZL184 (4, 8, and 16 mg/kg, IP) and **d–f** KML29 (4 and 16 mg/kg, IP) were administered 4 h before the tests. **a, d** Time spent in open arms (s); **b, e** time spent in closed arms (s); **c, f** anxiety index; Results are expressed as mean ± SEM ($n = 8$ per group). One-way ANOVA followed by Newman–Keuls multiple comparison test. *$P < 0.05$, **$P < 0.01$.

CB$_1$ receptor blockade fails to prevent the effects of JZL184

CB$_1$ receptors mediate the anxiolytic-like actions of JZL184 in mice or rats that are not exposed to a strong stressor prior to testing [15, 16]. To determine whether an analogous mechanism might operate in TMT-stressed rats, we measured anxiety-related behaviors in animals that had received a single maximally effective dose of the CB$_1$ inverse agonist rimonabant (1 mg/kg, IP) [6, 28] along with JZL184 (16 mg/kg, IP). When administered at this same dose to TMT-stressed rats, rimonabant abolished the anxiolytic-like effects of the FAAH inhibitor URB597 [22]. In striking contrast with those results, the drug failed to alter EPM behaviors in JZL184-treated rats (Fig. 2, Supplementary Table 1).

CB$_2$ receptors mediate the anxiolytic-like effects of JZL184 in TMT-exposed rats

CB$_2$ receptors have been implicated in the anxiolytic-like effects of JZL184 in mice [29]. We asked therefore whether a similar mechanism might also be operational in TMT-stressed rats. As shown in Fig. 3, administration of the CB$_2$ inverse agonist AM630 (5 mg/kg, IP; $n = 15$–16) [30] did not affect behavior in vehicle-treated animals, but abolished the changes produced by JZL184 (16 mg/kg, IP) on open arm time [AM630 effect F(1, 59) = 9.230; $P = 0.0035$; Interaction effect F(1, 59) = 12.49; $P = 0.0008$; Fig. 3a], open arm entries [AM630 effect F(1, 59) = 4.849; $P = 0.0316$; Interaction effect F (1, 59) = 7.916; $P = 0.0066$; Fig. 3b], anxiety index [AM630 effect F(1, 59) = 10.17; $P = 0.0023$; Interaction effect F (1, 59) = 12.43; $P = 0.0008$; Fig. 3c], stretch-attend postures [AM630 effect F(1, 59) = 7.980; $P = 0.0064$; Interaction

effect F (1, 59) = 10.26; $P = 0.0022$; Fig. 3d] and exploratory head dips [AM630 effect F (1, 59) = 6.008; $P = 0.0172$; Interaction effect F (1, 59) = 7.012; $P = 0.0104$; Fig. 3e].

If CB$_2$ receptors underpin the anxiolytic-like properties of JZL184, as the blockade by AM630 implies, direct-acting CB$_2$ agonists should also reduce fear-related behaviors. To test this, we administered ascending doses of the CB$_2$ agonist JWH133 [30] (0.3, 1 and 3 mg/kg, IP) or its vehicle to TMT-exposed rats, and subjected them to the EPM test 1 h later (n=8 per group). JWH133 elicited substantial anxiolytic-like effects at the dose of 3 mg/kg: open arm time [F (3, 28) = 5.451; $P = 0.0044$; Fig. 4a] open arm entries [F (3, 28) = 3.984; $P = 0.0175$; Fig. 4b] and EPM index (Supplementary Table 1) were increased, whereas the anxiety index was decreased [F (3, 28) = 4.632; $P = 0.0094$; Fig. 4c] by the treatment. Moreover, JWH133 reduced the number of stretch-attend postures ($P = 0.0069$) and increased the number of head dips ($P = 0.0488$) (not shown in figure). Confirming mediation by CB$_2$ receptors, the effects of JWH133 (3 mg/kg, IP) on open arm time [JWH133 effect F(1,28) = 15.07; $P = 0.0006$; Interaction effect F (1, 28) = 7.033; $P = 0.0130$; Fig. 4d], open arm entries [JWH133 effect F (1,28) = 11.27; $P = 0.0023$; Interaction effect F (1, 28) = 4.177; $P = 0.0505$; Fig. 4e] and anxiety and EPM indices [JWH133 effect F (1,28) = 8.207; $P = 0.0078$; Interaction effect F (1, 28) = 7.136; $P = 0.0124$; Fig. 4f, Supplementary Table 1] were suppressed by treatment with AM630 (5 mg/kg, IP) (n=8 per group). CB$_2$ blockade also partially or completely prevented the effects of JWH133 on stretch-attend postures ($P = 0.0781$) and head dips ($P = 0.0469$) (not shown in figure). Importantly, however, the CB$_2$
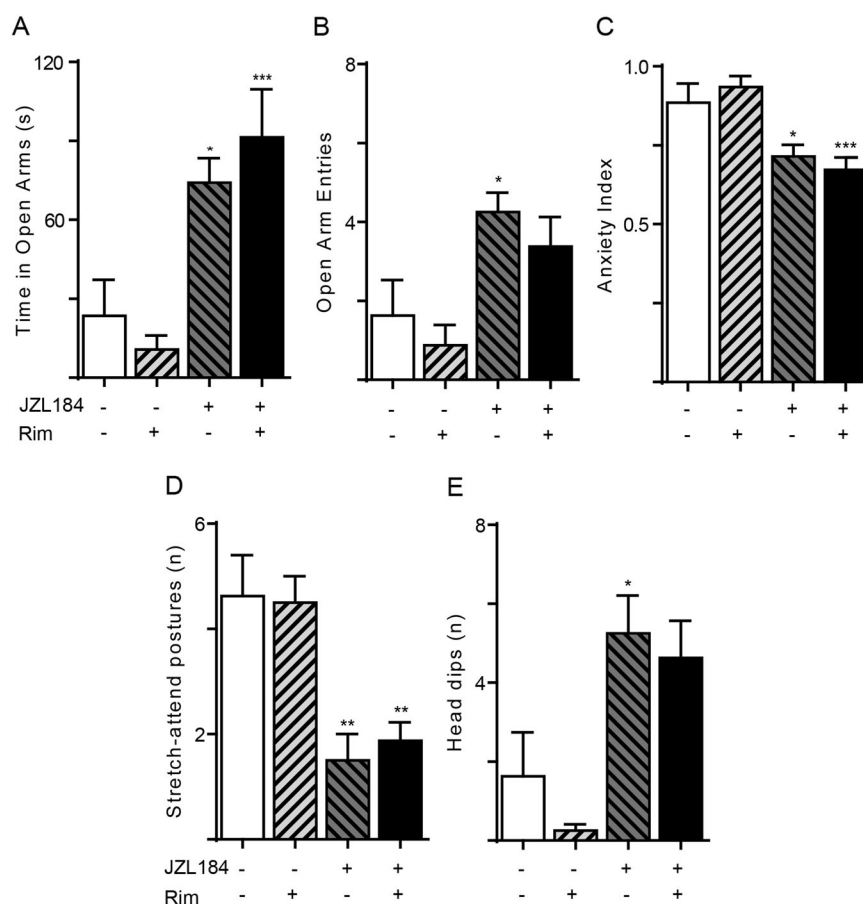
Fig. 2 CB$_1$ receptor antagonist rimonabant fails to prevent the anxiolytic-like effects of JZL184. The CB$_1$-selective inverse agonist rimonabant (rim, 1 mg/kg, IP) was administered together with JZL184 (16 mg/kg, IP) and rats were tested 4 h later. **a** Time spent in open arms (s); **b** number of open arm entries; **c** anxiety index; **d** number of stretch-attend postures; **e** number of head dips. Results are expressed as mean ± SEM ($n = 8$ per group). Two-way ANOVA followed by Newman–Keuls multiple comparison test. *$P < 0.05$, **$P < 0.01$, ***$P < 0.001$.

agonist failed to alter EPM measures in animals that had no prior experience of TMT (Fig. 4g–i). We interpret these findings as indicating that CB$_2$ activation – either by direct agonism or by elevation of endogenous 2-AG – alleviates fear-related behaviors in TMT-stressed, but not TMT-naïve rats.

TMT exposure increases CB$_2$ mRNA levels in prefrontal cortex
The expression of CB$_2$ receptors can be induced by a variety of pathological stimuli [31]. To test whether predator stress might be one such stimulus, we measured transcription of the *Cnr2* gene (which encodes for CB$_2$ in rodents) in various regions of the rat brain 7 days after exposure to TMT or its vehicle (n = 8 per group). In parallel, *Cnr1* (CB$_1$) mRNA levels were also assessed. At the time of euthanasia, blood constituents that are known to contain CB$_1$ and CB$_2$ receptors were removed from the cerebral circulation by saline perfusion. Quantitative RT-PCR analyses showed that TMT exposure increased *Cnr2* transcription in extracts of prefrontal cortex ($t(14) = 5.812$; $P = 0.0003$), but not cerebellum, striatum, hypothalamus, hippocampus or amygdala (Fig. 5a). By contrast, no statistically detectable change in *Cnr1* mRNA levels was observed in any of the regions surveyed (Fig. 5b).

DISCUSSION
The present study set out to investigate the impact of systemic MGL inhibition in the rat TMT model of innate predator-induced fear, which reproduces some features of human post-traumatic stress disorder (PTSD) [21, 32]. At the outset, we expected that

blockade of intracellular MGL activity by the compound JZL184 would attenuate fear-related responses in a CB$_1$ receptor-dependent manner, as reported for other rodent models of anxiety [15–17]. This prediction was only partially borne out by the data. Indeed, even though JZL184 exerted substantial anxiolytic-like effects in TMT-stressed rats, these were suppressed by CB$_2$ – not CB$_1$ – antagonism. Two lines of evidence provided further support for an involvement of CB$_2$ receptors. First, following exposure to predator stress there was a persistent increase in CB$_2$ gene transcription in the prefrontal cortex – a brain region implicated in inhibitory control and affect [33, 34]. Additionally, the selective CB$_2$ agonist JWH133 attenuated fear responses in TMT-exposed but not TMT-naïve animals. Together, the results suggest that a single ethologically relevant traumatic event (i.e., unprotected exposure to a predator) may promote the emergence of a defensive CB$_2$-dependent mechanism, driven by endogenously produced 2-AG, which might modulate the adaptive response to the trauma.

Multiple studies have shown that the anxiolytic-like effects of FAAH and MGL inhibitors are rooted in the indirect activation of CB$_1$ receptors via accrued endocannabinoid signaling [15–17]. By contrast, evidence for a role of CB$_2$ in such effects is still sparse and somewhat contradictory. Busquets-Garcia et al. showed that JZL184 (8 mg/kg, IP) exerted anxiolytic-like effects in the mouse EPM test, which were prevented by pharmacological antagonism or genetic deletion of CB$_2$ receptors, and were mimicked by the CB$_2$ agonist JWH133 [29]. Consistent with those findings, García-Gutiérrez and Manzanares reported that mice constitutively
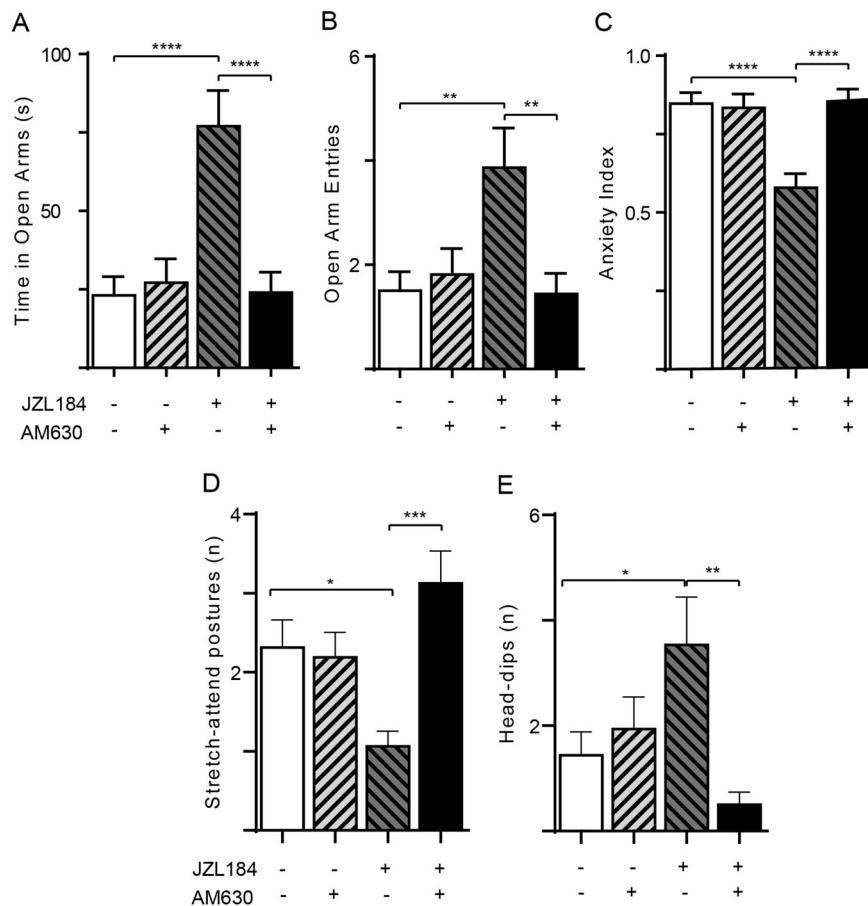
Fig. 3 CB2 receptor antagonist AM630 prevents the anxiolytic-like effects of JZL184. The CB$_2$-selective inverse agonist AM630 (5 mg/kg, IP) was administered 3 h after JZL184 (16 mg/kg, IP) and 1 h before behavioral testing. **a** Time spent in open arms (s); **b** number of open arm entries; **c** anxiety index; **d** number of stretch-attend postures; **e** number of head dips. Results are expressed as mean ± SEM ($n = 15$–16 per group). Two-way ANOVA followed by Newman–Keuls multiple comparison test. *$P < 0.05$, **$P < 0.01$, ***$P < 0.001$.

overexpressing CB$_2$ displayed lower anxiety-related responses in the EPM and light-dark box tests, compared to their wild-type littermates [35]. Another study failed, however, to confirm the anxiolytic-like properties of JWH133 [35] while yet another showed that a structurally distinct CB$_2$ agonist did not affect marble-burying behavior in mice [36]. Mouse strain differences might account for some of these discrepant findings, but our experiments point to environmental stress as an additional contributor. We found that exposing rats to TMT enhanced *Cnr2* (but not *Cnr1*) transcription in rat prefrontal cortex (Fig. 5a) while concomitantly unmasking an anxiolytic-like action of JWH133 that is undetectable in TMT-naïve animals (Fig. 4g–i). These results underscore the diverse roles played by the endocannabinoid system in stress-coping behaviors, as well as the need to carefully control stress-related variables when investigating such roles.

We showed that severe stress triggers CB$_2$ gene transcription in select regions of the rat brain. This is consistent with the highly inducible nature of the receptor [31], whose transcriptional activation by a variety of pathological signals is well documented [29, 37–42]. We did not attempt to identify the cell type(s) that up-regulate CB$_2$ when rats are exposed to TMT, but possible candidates include not only resident constituents of the brain – such as neurons [43] and microglia [24, 44] – but also blood-borne immune cells that may infiltrate the CNS in response to stress. Indeed, TMT-exposed rats develop a systemic inflammatory state [45, 46] that may facilitate the trafficking of circulating monocytes into the brain, where these CB$_2$-expressing cells might influence affect and mood through the release

of anxiogenic cytokines such as interleukin 1β (IL-1β) and tumor necrosis factor (TNF)-α [47, 48]. Supporting this possibility, it has been shown that CB$_2$ activation inhibits monocyte secretion of IL-1β and TNF-α [49], and impairs the cells' ability to interact with the cerebral endothelium and to migrate across the blood-brain barrier [50, 51].

The FAAH inhibitor URB597 exerts profound anxiolytic-like effects in rat models of persistent fear-related behaviors evoked by psychological trauma [22, 52, 53]. For example, Fidelman et al. showed that administration of low doses of the compound (≤1 mg/kg) normalized startle response and extinction kinetics in rats that had received a combination of inescapable foot shock and situational reminders [52]. Similarly, we previously reported that URB597 (≤1 mg/kg) suppressed behavioral correlates of anxiety in rats exposed to TMT [22]. In both studies, CB$_1$ receptor blockade completely prevented the effects of FAAH inhibition. The available data thus indicate that anandamide-mediated signaling at CB$_1$ may modulate the long-term consequences of trauma. Further expanding the roles of the endocannabinoid system in stress modulation, the present results suggest that life-threatening events may cause the emergence of a second defensive mechanism – dependent on 2-AG-mediated engagement of newly recruited CB$_2$ receptors – which might act in concert with anandamide-mediated CB$_1$ activation to enhance stress-coping behaviors.

The translational relevance of our findings is limited by the validity of the TMT model, which does not capture the complexity of human PTSD [54]. Beside anxiety and systemic inflammation, which are reproduced by exposure to the predator odor
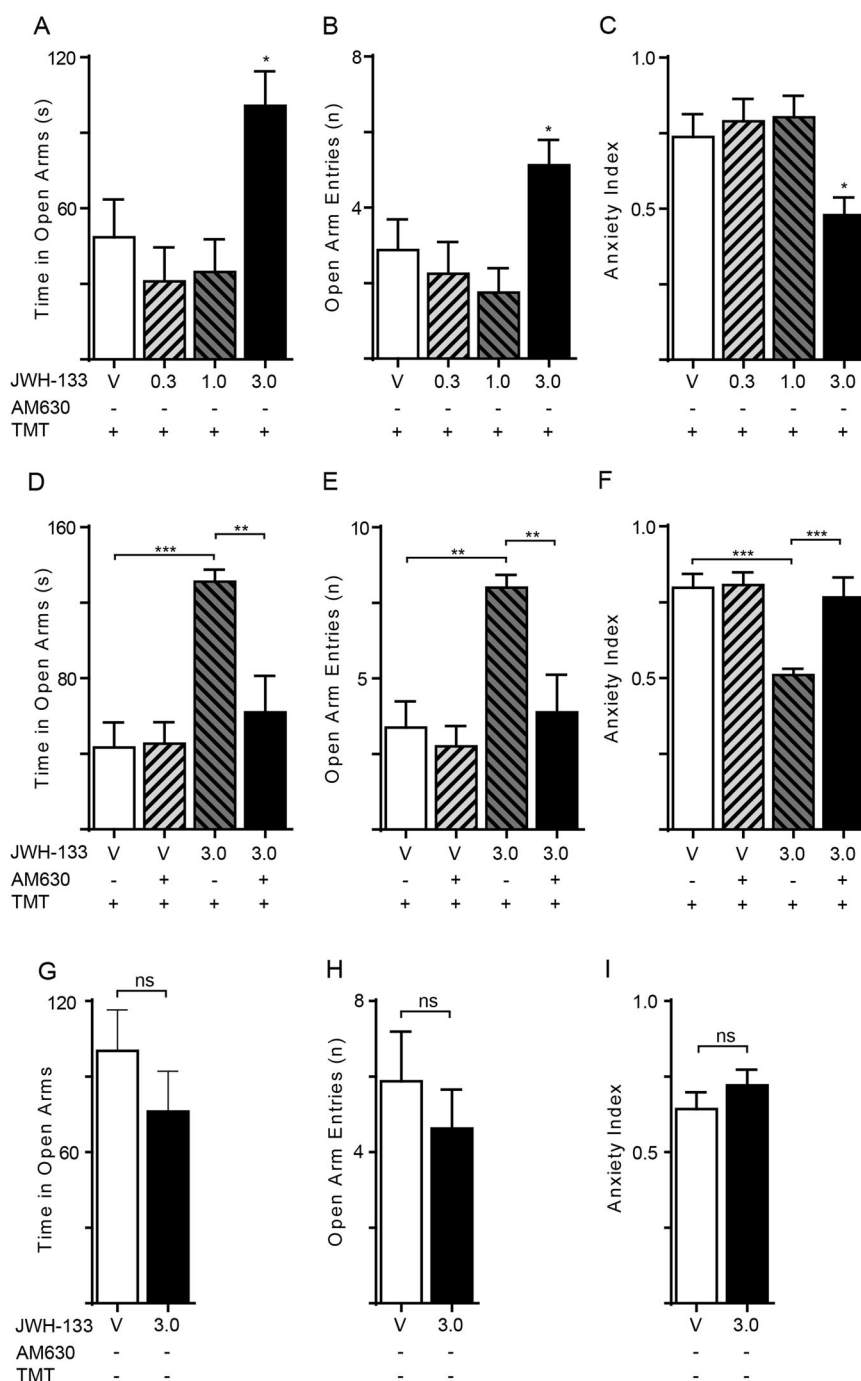
Fig. 4 Effects of CB$_2$ agonist JWH133 on anxiety-related behaviors in TMT-stressed rats. The CB$_2$-selective agonist JWH133 (0.3, 1 and 3 mg/kg, IP) was administered 1 h before the tests. TMT-stressed rats: (**a**) Time spent in open arms (s); (**b**) number of open arm entries; (**c**) anxiety index; One-way ANOVA followed by Newman–Keuls multiple comparison test. *$P < 0.05$, **$P < 0.01$, ***$P < 0.001$. Emotionally naïve rats: (**d**) Time spent in open arms (s); (**e**) number of open arm entries; (**f**) anxiety index; Two-way ANOVA followed by Newman–Keuls multiple comparison test. *$P < 0.05$, **$P < 0.01$, ***$P < 0.001$. TMT-exposed rats treated with the CB$_2$ inverse agonist AM630 (5 mg/kg, IP): (**g**) Time spent in open arms (s); (**h**) number of open arm entries; (**i**) anxiety index; Student's t test with Bonferroni's correction. Results are expressed as mean ± SEM ($n = 8$ per group).

[20, 21, 46], persons with PTSD experience a variety of symptoms – including intrusive trauma memories, avoidance of trauma reminders, hyperarousal and nightmares [32] – that no available animal paradigm incorporates. A recent human genetic study suggests, however, that impaired CB$_2$ activity may contribute to PTSD pathogenesis [55]. Investigating a cohort of 921 volunteers from the general population, Lazary and collaborators examined whether the non-synonymous R63Q polymorphism of the CB$_2$ gene (*CNR2*), which encodes for a hypofunctional form of the receptor [56], might be associated with symptoms of anxiety and depression. The analysis revealed a significant interaction between R63Q and negative affective consequences of childhood trauma. Though additional work is needed to confirm this link, the available evidence does support the hypothesis, suggested by our
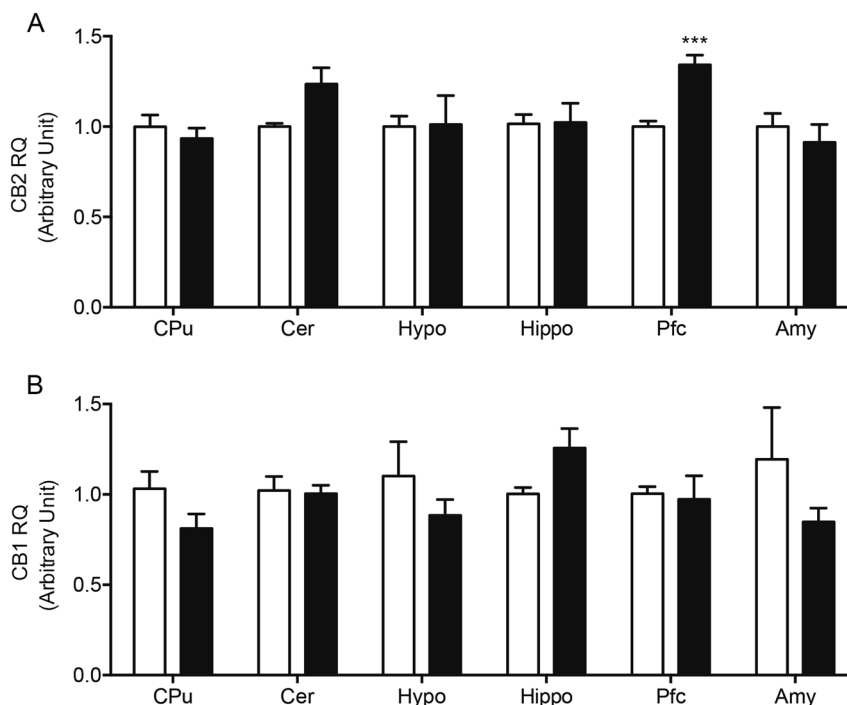
Fig. 5 Effects of TMT exposure on CB$_2$ (*Cnr2*) and CB$_1$ (*Cnr1*) transcription in various regions of the rat brain. *Cnr2* and *Cnr1* mRNA levels were measured by quantitative RT-PCR 1 week after exposure to TMT. **a** *Cnr2* mRNA levels; **b** *Cnr1* mRNA levels. Vehicle, open bars; TMT, closed bars. CPu caudate putamen, Cer cerebellum, Hypo hypothalamus, Hippo hippocampus, Pfc prefrontal cortex, Amy amygdala. Results are expressed as mean ± SEM ($n = 8$ per group). Student's t test with Bonferroni's correction; *$P < 0.0083$, ***$P < 0.001$.

results, that 2-AG-mediated CB$_2$ activation may serve as an adaptive signal that attenuates the affective sequelae of life trauma.

CONCLUSIONS
PTSD is a frequent and severe psychiatric condition for which few therapeutic options are available [57]. The present study identifies MGL-regulated 2-AG signaling at CB$_2$ receptors as an anti-stress mechanism activated by psychological trauma, and as a potential target for PTSD drug discovery.

AUTHOR CONTRIBUTIONS
DI participated in the design of the study, performed experiments and wrote a first draft of the manuscript. FP participated in experiments and in the writing of the manuscript and revision. VV contributed in the design of the study and performed experiments. YF performed experiments required in the revision. AY and GR scored the EPM videos. DM and GW participated in the design of the study. DP ideated and designed the study, and wrote the manuscript.

ADDITIONAL INFORMATION
Supplementary Information accompanies this paper at (https://doi.org/10.1038/s41386-020-0696-x).

Publisher's note Springer Nature remains neutral with regard to jurisdictional claims in published maps and institutional affiliations.

REFERENCES
1. Patel S, Hill MN, Cheer JF, Wotjak CT, Holmes A. The endocannabinoid system as a target for novel anxiolytic drugs. Neurosci Biobehav Rev. 2017;76:56–66.
2. Piomelli D. The molecular logic of endocannabinoid signalling. Nat Rev Neurosci. 2003;4:873–84.
3. Di Marzo V. New approaches and challenges to targeting the endocannabinoid system. Nat Rev Drug Disco. 2018;17:623–39.
4. Kathuria S, Gaetani S, Fegley D, Valiño F, Duranti A, Tontini A, et al. Modulation of anxiety through blockade of anandamide hydrolysis. Nat Med. 2003;9:76–81.
5. Tarzia G, Duranti A, Tontini A, Piersanti G, Mor M, Rivara S, et al. Design, synthesis, and structure - activity relationships of alkylcarbamic acid aryl esters, a new class of fatty acid amide hydrolase inhibitors. J Med Chem. 2003;46:2352–60.
6. Gobbi G, Bambico FR, Mangieri R, Bortolato M, Campolongo P, Solinas M, et al. Antidepressant-like activity and modulation of brain monoaminergic transmission by blockade of anandamide hydrolysis. Proc Natl Acad Sci USA. 2005;102:18620–5.
7. Naidu PS, Varvel SA, Ahn K, Cravatt BF, Martin BR, Lichtman AH. Evaluation of fatty acid amide hydrolase inhibition in murine models of emotionality. Psychopharmacol (Berl). 2007;192:61–70.
8. Haller J, Barna I, Barsvari B, Gyimesi Pelczer K, Yasar S, Panlilio LV, et al. Interactions between environmental aversiveness and the anxiolytic effects of enhanced cannabinoid signaling by FAAH inhibition in rats. Psychopharmacol (Berl). 2009;204:607–16.
9. Bortolato M, Mangieri RA, Fu J, Kim JH, Arguello O, Duranti A, et al. Antidepressant-like activity of the fatty acid amide hydrolase inhibitor URB597 in a rat model of chronic mild stress. Biol Psychiatry. 2007;62:1103–10.
10. Mayo LM, Asratian A, Lindé J, Morena M, Haataja R, Hammar V, et al. Elevated anandamide, enhanced recall of fear extinction, and attenuated stress responses following inhibition of fatty acid amide hydrolase: a randomized, controlled experimental medicine trial. Biol Psychiatry. 2019;87:538–47.

11. Mayo LM, Asratian A, Lindé J, Holm L, Nätt D, Augier G, et al. Protective effects of elevated anandamide on stress and fear-related behaviors: translational evidence from humans and mice. Mol Psychiatry. 2018;25:993–1005.

12. Katona I, Freund TF. Multiple functions of endocannabinoid signaling in the brain. Annu Rev Neurosci. 2012;35:529–58.

13. Dinh TP, Carpenter D, Leslie FM, Freund TF, Katona I, Sensi SL, et al. Brain monoglyceride lipase participating in endocannabinoid inactivation. Proc Natl Acad Sci USA. 2002;99:10819–24.

14. Gulyas AI, Cravatt BF, Bracey MH, Dinh TP, Piomelli D, Boscia F, et al. Segregation of two endocannabinoid-hydrolyzing enzymes into pre- and postsynaptic compartments in the rat hippocampus, cerebellum and amygdala. Eur J Neurosci. 2004;20:441–58.

15. Sciolino NR, Zhou W, Hohmann AG. Enhancement of endocannabinoid signaling with JZL184, an inhibitor of the 2-arachidonoylglycerol hydrolyzing enzyme monoacylglycerol lipase, produces anxiolytic effects under conditions of high environmental aversiveness in rats. Pharm Res. 2011;64:226–34.

16. Kinsey SG, O'Neal ST, Long JZ, Cravatt BF, Lichtman AH. Inhibition of endocannabinoid catabolic enzymes elicits anxiolytic-like effects in the marble burying assay. Pharm Biochem Behav. 2011;98:21–7.

17. Lim J, Igarashi M, Jung KM, Butini S, Campiani G, Piomelli D. Endocannabinoid modulation of predator stress-induced long-term anxiety in rats. Neuropsychopharmacology. 2016;41:1329–39.

18. Almeida-Santos AF, Gobira PH, Rosa LC, Guimaraes FS, Moreira FA, Aguiar DC. Modulation of anxiety-like behavior by the endocannabinoid 2-arachidonoylglycerol (2-AG) in the dorsolateral periaqueductal gray. Behav Brain Res. 2013;252:10–7.

19. Scarante FF, Vila-Verde C, Detoni VL, Ferreira-Junior NC, Guimarães FS, Campos AC. Cannabinoid modulation of the stressed hippocampus. Front Mol Neurosci. 2017;10:411.

20. Wallace KJ, Rosen JB. Predator odor as an unconditioned fear stimulus in rats: elicitation of freezing by trimethylthiazoline, a component of fox feces. Behav Neurosci. 2000;114:912–22.

21. Rosen JB, Asok A, Chakraborty T. The smell of fear: innate threat of 2,5-dihydro-2,4,5-trimethylthiazoline, a single molecule component of a predator odor. Front Neurosci. 2015;9:292.

22. Danandeh A, Vozella V, Lim J, Oveisi F, Ramirez GL, Mears D, et al. Effects of fatty acid amide hydrolase inhibitor URB597 in a rat model of trauma-induced long-term anxiety. Psychopharmacol (Berl). 2018;235:3211–21.

23. Gaetani S, Oveisi F, Piomelli D. Modulation of meal pattern in the rat by the anorexic lipid mediator oleoylethanolamide. Neuropsychopharmacology. 2003;28:1311–6.

24. Stella N. Cannabinoid and cannabinoid-like receptors in microglia, astrocytes, and astrocytomas. Glia. 2010;58:1017–30.

25. Pan B, Wang W, Long JZ, Sun D, Hillard CJ, Cravatt BF, et al. Blockade of 2-arachidonoylglycerol hydrolysis by selective monoacylglycerol lipase inhibitor 4-nitrophenyl 4-(dibenzo[d] [1,3]dioxol-5-yl(hydroxy)methyl) piperidine-1-carboxylate (JZL184) enhances retrograde endocannabinoid signaling. J Pharm Exp Ther. 2009;331:591–7.

26. Long JZ, Nomura DK, Cravatt BF. Characterization of monoacylglycerol lipase inhibition reveals differences in central and peripheral endocannabinoid metabolism. Chem Biol. 2009;16:744–53.

27. Ignatowska-Jankowska BM, Ghosh S, Crowe MS, Kinsey SG, Niphakis MJ, Abdullah RA, et al. In vivo characterization of the highly selective monoacylglycerol lipase inhibitor KML29: antinociceptive activity without cannabimimetic side effects. Br J Pharm. 2014;171:1392–407.

28. Wei LW, Yuan ZQ, Zhao MD, Gu CW, Han JH, Fu L. Inhibition of cannabinoid receptor 1 can influence the lipid metabolism in mice with diet-induced obesity. Biochem. 2018;83:1279–87.

29. Busquets-Garcia A, Puighermanal E, Pastor A, De La Torre R, Maldonado R, Ozaita A. Differential role of anandamide and 2-arachidonoylglycerol in memory and anxiety-like responses. Biol Psychiatry. 2011;70:479–86.

30. Soethoudt M, Grether U, Fingerle J, Grim TW, Fezza F, De Petrocellis L, et al. Cannabinoid CB$_2$ receptor ligand profiling reveals biased signalling and off-target activity. Nat Commun. 2017;8:13958.

31. Hu SS, Mackie K. Distribution of the endocannabinoid system in the central nervous system. Handb Exp Pharm. 2015;231:59–93.

32. Earle WJ. DSM-5. Philos Forum; Berlin, Germany, 2014.

33. Andrewes DG, Jenkins LM. The role of the amygdala and the ventromedial prefrontal cortex in emotional regulation: implications for post-traumatic stress disorder. Neuropsychol Rev. 2019;29:220–43.

34. Goode TD, Maren S. Common neurocircuitry mediating drug and fear relapse in preclinical models. Psychopharmacol (Berl). 2019;236:415–37.

35. García-Gutiérrez MS, Manzanares J. Overexpression of CB$_2$ cannabinoid receptors decreased vulnerability to anxiety and impaired anxiolytic action of alprazolam in mice. J Psychopharmacol. 2011;25:111–20.

36. Valenzano KJ, Tafesse L, Lee G, Harrison JE, Boulet JM, Gottshall SL, et al. Pharmacological and pharmacokinetic characterization of the cannabinoid receptor 2 agonist, GW405833, utilizing rodent models of acute and chronic pain, anxiety, ataxia and catalepsy. Neuropharmacology. 2005;48:658–72.

37. Sánchez C, de Ceballos ML, Gomez del Pulgar T, Rueda D, Corbacho C, Velasco G, et al. Inhibition of glioma growth in vivo by selective activation of the CB(2) cannabinoid receptor. Cancer Res. 2001;61:5784–9.

38. Benito C, Núñez E, Tolón RM, Carrier EJ, Rábano A, Hillard CJ, et al. Cannabinoid CB$_2$ receptors and fatty acid amide hydrolase are selectively overexpressed in neuritic plaque-associated glia in Alzheimer's disease brains. J Neurosci. 2003;23:11136–41.

39. Benito C, Romero JP, Tolón RM, Clemente D, Docagne F, Hillard CJ, et al. Cannabinoid CB$_1$ and CB$_2$ receptors and fatty acid amide hydrolase are specific markers of plaque cell subtypes in human multiple sclerosis. J Neurosci. 2007;27:2396–402.

40. Yiangou Y, Facer P, Durrenberger P, Chessell IP, Naylor A, Bountra C, et al. COX-2, CB$_2$ and P2X7-immunoreactivities are increased in activated microglial cells/macrophages of multiple sclerosis and amyotrophic lateral sclerosis spinal cord. BMC Neurol. 2006;6:12.

41. Onaivi ES, Ishiguro H, Sejal P, Meozzi PA, Myers L, Tagliaferro P, et al. Methods to study the behavioral effects and expression of CB$_2$ cannabinoid receptor and its gene transcripts in the chronic mild stress model of depression. Methods Mol Med. 2006;123:291–8.

42. Robertson JM, Achua JK, Smith JP, Prince MA, Staton CD, Ronan PJ, et al. Anxious behavior induces elevated hippocampal CB$_2$ receptor gene expression. Neuroscience. 2017;352:273–84.

43. Jordan CJ, Xi ZX. Progress in brain cannabinoid CB$_2$ receptor research: from genes to behavior. Neurosci Biobehav Rev. 2019;98:208–20.

44. Walter L, Franklin A, Witting A, Wade C, Xie Y, Kunos G, et al. Nonpsychotropic cannabinoid receptors regulate microglial cell migration. J Neurosci. 2003;23:1398–405.

45. Holman EA, Guijarro A, Lim J, Piomelli D. Effects of acute stress on cardiac endocannabinoids, lipogenesis, and inflammation in rats. Psychosom Med. 2014;76:20–8.

46. Mellon SH, Gautam A, Hammamieh R, Jett M, Wolkowitz OM. Metabolism, metabolomics, and inflammation in posttraumatic stress disorder. Biol Psychiatry. 2018;83:866–75.

47. Kho DT, Glass M, Graham ES. Is the cannabinoid CB$_2$ receptor a major regulator of the neuroinflammatory axis of the neurovascular unit in humans? Adv Pharm. 2017;80:367–96.

48. Deslauriers J, Powell SB, Risbrough VB. Immune signaling mechanisms of PTSD risk and symptom development: insights from animal models. Curr Opin Behav Sci. 2017;14:123–32.

49. Klegeris A, Bissonnette CJ, McGeer PL. Reduction of human monocytic cell neurotoxicity and cytokine secretion by ligands of the cannabinoid-type CB$_2$ receptor. Br J Pharm. 2003;139:775–86.

50. Ramirez SH, Haskó J, Skuba A, Fan S, Dykstra H, McCormick R, et al. Activation of cannabinoid receptor 2 attenuates leukocyte-endothelial cell interactions and blood-brain barrier dysfunction under inflammatory conditions. J Neurosci. 2012;32:4004–16.

51. Rom S, Zuluaga-Ramirez V, Dykstra H, Reichenbach NL, Pacher P, Persidsky Y. Selective activation of cannabinoid receptor 2 in leukocytes suppresses their engagement of the brain endothelium and protects the blood-brain barrier. Am J Pathol. 2013;183:1548–58.

52. Fidelman S, Mizrachi Zer-Aviv T, Lange R, Hillard CJ, Akirav I. Chronic treatment with URB597 ameliorates post-stress symptoms in a rat model of PTSD. Eur Neuropsychopharmacol. 2018;28:630–42.

53. Morena M, Berardi A, Colucci P, Palmery M, Trezza V, Hill MN, et al. Enhancing endocannabinoid neurotransmission augments the efficacy of extinction training and ameliorates traumatic stress-induced behavioral alterations in rats. Neuropsychopharmacology. 2018;43:1284–96.

54. Richter-Levin G, Stork O, Schmidt MV. Animal models of PTSD: a challenge to be met. Mol Psychiatry. 2018;24:1135–56.

55. Lazary J, Eszlari N, Juhasz G, Bagdy G. A functional variant of CB$_2$ receptor gene interacts with childhood trauma and FAAH gene on anxious and depressive phenotypes. J Affect Disord. 2019;257:716–22.

56. Ishiguro H, Carpio O, Horiuchi Y, Shu A, Higuchi S, Schanz N, et al. A non-synonymous polymorphism in cannabinoid CB$_2$ receptor gene is associated with eating disorders in humans and food intake is modified in mice by its ligands. Synapse. 2010;64:92–6.

57. Sartori SB, Singewald N. Novel pharmacological targets in drug development for the treatment of anxiety and anxiety-related disorders. Pharm Ther. 2019;204:107402.